MAPPING SUPRAGLACIAL DEBRIS FROM THE SCHIRMACHER OASIS, EAST ANTARCTICA USING MATLAB IMAGE PROCESSING TOOLBOX

Shridhar D. Jawak[1], Anirudh T.S.[2], Alvarinho J. Luis[1]
[1]Polar Remote Sensing Section, Polar Sciences Group, Earth System Science Organization (ESSO), National Centre for Antarctic and Ocean Research (NCAOR), Ministry of Earth Sciences (MoES), Government of India, Headland Sada, Vasco-da-Gama, Goa─403804, India, Email: shridhar.jawak@gmail.com, alvluis1@gmail.com
[2]Indian Institute of Information Technology and Management, Kerala─695581, India. Email: anisomadas@gmail.com

KEYWORDS: Supraglacial debris; optical satellite imagery; MATLAB

ABSTRACT

In this study, we performed pixel-based characterization of supraglacial debris on Schirmacher Oasis, Princess Astrid Coast, Queen Maud Land, East Antarctica, using high-resolution WorldView-2 (WV-2) satellite imagery. Schirmacher Oasis is covered with blue ice, white ice, and snow. Debris being an important parameter in glacial melt and ablation, pixel-based methods were employed using MATLAB image processing routines. The results suggest that pixel-based methods yielded around 70% accuracy, when compared to manual reference. Results with MATLAB looks promising with subdued over and under estimation when compared with the manual area (debris area). Accuracy assessment for the classification was done using manually digitized reference data with the help of confusion matrix. Future attempts include analyzing the distribution with respect to altitude, presence of streams and temporal change in the distribution on different years.

1. INTRODUCTION

Debris on the surface of the glacier is known as supraglacial moraine or supraglacial debris. It is a product of weathering processes that occur during melt-refreeze cycles. Supra glacial debris is widely spread in many high relief areas and has substantial influence on glacier behavior, debris can accelerate (if thin) or suppress (if thick) glacier melt beneath the debris relative to clean ice. Because debris covered glaciers usually contains large ice volumes (Müller and Scherler, 1966) Data regarding distribution of debris that can be incorporated into glacier models is a key for improving accuracy of current glacier models. Glacier melting below the debris is controlled by 3 major factors; spatial distribution of debris, thickness of debris, and thermal conductivity of debris. Several existing glacier mass balance models have successfully represented ice melting under debris (Juen et al., 2014). This study is focused on usage of high-resolution satellite imagery for semiautomatic extraction and mapping of supra glacial debris (Jawak et al., 2016b) on a relatively larger area. We used pan sharpened 8 band multispectral data from digital globe's WorldView-2 (WV-2) satellite with 0.46 m resolution Panchromatic band and 1.84 m resolution for multispectral resolution (Jawak et al., 2015a; Jawak et al., 2015b) . Low and medium resolution satellite images are frequently used for environmental monitoring in remote areas around the globe but these satellites cannot provide detailed spatial and spectral information in cryosphere regions. Satellites like Landsat, AVHRR, IKONOS have been successfully used to produce Antarctic land cover maps but the resulting thematic maps exhibited low classification accuracy because of the less number of bands and special resolution (Jawak et al., 2015c). Jawak and Luis (2012) evaluated the potential of 8-band HR WorldView-2 (WV-2) panchromatic (PAN) and multispectral image (MSI) data for the extraction of polar geospatial information. The authors have mapped the Larsemann Hills of Eastern Antarctica into the three most abundant land cover classes—snow/ice, water bodies, and landmasses, using customized normalized difference spectral index ratios on WV-2 images. An overall accuracy of 95 to 98% was achieved with this procedure. Jawak and Luis (2012) have also compared four different image classification methods to improve the accuracy of the cryosphere land cover mapping from VHR WV-2 satellite images of Larsemann Hills, east Antarctica. The images on which the authors performed the classification techniques were made up of eight-band MSIs and PAN WV-2 images fused using the hyper spherical color sharpening method. Three classes of land cover—land mass/rocks, water/lakes, and snow/ice—were classified using identical training samples. They used four distinctly different pixel-by-pixel classification methods to classify the WV-2 PAN-sharpened data: a SVM, MXL, NNC, and SAM and then integrated the final thematic land cover map of Larsemann Hills, east Antarctica, using ensemble classification based on a majority voting–coupled WTA approach. In this study, we focused our research on mapping supraglacial debris in Schirmacher oasis, Antarctica using simple pixel based methods using MATLAB. We performed accuracy assessment with the help of 16 sample tiles selected based on different criteria's like altitude presence of streams etc.

2. STUDY AREA AND DATA

We used 11-bit WV-2 data (ortho-rectified and radiometrically corrected) in this study. It has 8 bands and out of which Red Edge, Yellow, Coastal and NIR2 facilitated high precision on spectral analysis for land use/land cover mapping cryospheric information extraction, visualization and simulation environments, and bathymetry derivations. The spectral and spatial range of various bands of WV-2 are depicted in Table 1. In this study, the spectral characteristics of the supraglacial debris in the Antarctic environment from the hyper-spatial WorldView-2 images were analyzed by utilizing a combination of RS techniques. The WV-2 images were acquired over the Schirmacher oasis on 05 February 2012 (Figure 1). The ground reference datasets used to support supraglacial debris mapping is the digitized data from pan sharpened WV-2 images. Antarctica is known as the 'ice desert' but in this icy continent there are areas which are ice free and they are called as Oases, they occur at the edge of ice sheet zones or sometimes oases occupy such large areas including large number of lakes, ponds . Schirmacher oasis or Schirmacher lake plateau is a 28 km long and up to 3 km wide ice-free plateau containing more than 100 freshwater lakes. It is situated in the Princess Astrid Coast in Queen Maud Land in east Antarctica (100 meters above sea level), Antarctic ice sheet south of Schirmacher oasis reaches heights of 1500 m. Between the offshore ice sheet and Wegner Ice Sheet Plateau are the Wohlthat Mountains. Schirmacher oasis has a relatively mild climate compared to Antarctic conditions annual average temperature is −10.4 °C, annual average wind speed is 9.7 m/s, annual average precipitation is 264.5 mm there are around 350 hours of sunlight per month. Because of its positive radiation balance, the Schirmacher Oasis is regionally classified as a 'coastal climate zone'.

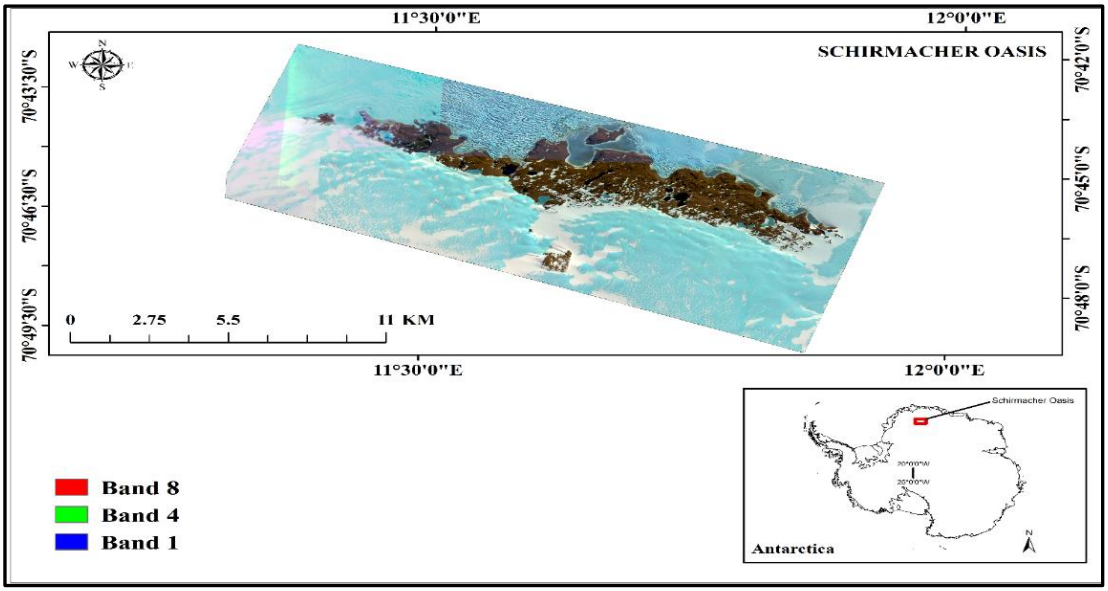

Figure 1. Location of Schirmacher Oasis in Antarctica

Table 1. Spatial and spectral range of bands of WorldView-2 satellite imagery

WV2- Bands	Band Name	Wavelength(µm)	Pixel size (m)
PAN	Panchromatic	0.450 - 0.800	0.5
Band 1	Coastal	0.400 - 0.450	2
Band 2	Blue	0.450 - 0.510	2
Band 3	Green	0.510 - 0.580	2
Band 4	Yellow	0.585 - 0.625	2
Band 5	Red	0.630 - 0.690	2
Band 6	Red Edge	0.705 – 0.745	2
Band 7	NIR-1	0.770 – 0.895	2
Band 8	NIR-2	0.860 – 1.040	2

3. METHODOLOGY

Protocol followed for extraction of debris is shown in figure 2. It contains 3 parts (i) Data preprocessing and pan sharpening, (ii) Preparation of reference data through manual digitization, (iii) Extraction using MATLAB and

accuracy assessment. We implemented DOS (Dark object subtractions) and QUAC (Quick atmospheric correction) for data calibration (Lillesand R.W., 2015) Dark object subtraction was performed to reduce path radiance from each band. Atmospheric correction is a major issue in Visible to NIR (VNIR) remote sensing (RS) because the atmosphere always influences radiation from ground to the sensor. However, the effects of atmospheric particles through absorption and scattering of the radiation from the earth surface contaminate the large amounts of imagery collected by the satellites. The severe effect that atmosphere has on visible and NIR radiance is it modifies spectral and spatial distribution of the radiation incident on the surface. The dark object is the minimum digital number (DN) value for more than 1000 pixels over the whole image (Jawak et al., 2016a) We utilized clear lakes as dark objects in our analysis. We implemented the QUAC model embedded in ENVI software in order to obtain prominent results for atmospheric correction. This method is used for MS and hyperspectral imagery that works with visible and NIR through SWIR wavelength range. It determines atmospheric correction parameters directly from the observed pixel spectra in an image. QUAC is based on the empirical finding that the average reflectance of diverse material spectra is not dependent on each image. The data calibration procedure was carried out with two steps, converting raw DN values to at-sensor spectral radiance factors and converting spectral radiance to top-of-atmosphere reflectance (TOA) (Jawak and Matthew, 2011; Jawak and Luis, 2012; Jawak et al., 2013a; Jawak and Luis 2013b; Jawak et al., 2013c; Jawak et al., 2013d; Jawak et al., 2013e; Jawak and Luis, 2014a; Jawak and Luis 2014b; Jawak et al., 2014c; Jawak and Luis, 2014d; Jawak and Luis, 2015d; Jawak and Luis, 2015e; Jawak et al; 2015f).

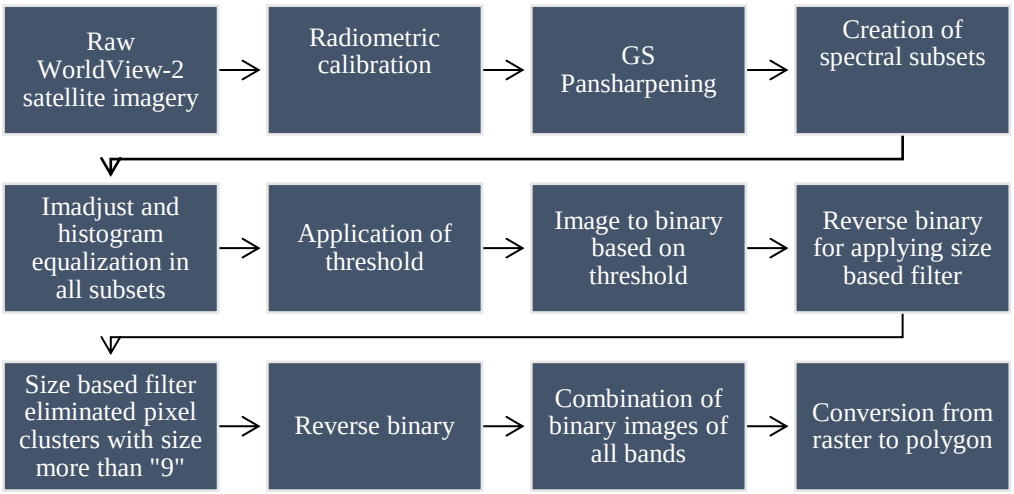

Figure 2. Methodology

For classification we used from functions from MATLAB's image processing toolbox. Separate thresholds was applied to each band, Band 1 (0.7-0.89), Band 4 (0.28 – 0.31), Band 6 (0.68) played major role in extraction of debris. Other bands like Band 2 (0.8 – 0.82), Band 3 (0.3 – 0.33), Band 5 (0.76), Band 7 (0.48), Band 8 (0.36) helped to distinguish elements which has similar size and shape e.g. shadows, parts of streams etc. *Imadjust* increases the contrast of the output image. It was performed for better visibility. Each band was read separately and thresholds were applied to create a binary image that included only debris in it. Binary files from each band were added together and a size based filter was applied to avoid shadows and other large areas. Values in each band range from 0 to 1 and we found that band 1, 4 & 6 played a major role in extracting debris. For applying size based filter *Imbinarize* tool from MATLAB's image processing toolbox was used. *Imbinarize* function is used for converting image to binary where debris appears in black color and the rest in white, in some parts of the image shadows were also classified as debris. Those shadows appeared as long chain of black pixels. To eliminate such chain like clusters a size based filter is used. Size based filter only works in white pixels (with value 1), therefore an inverted binary image was created (Debris in white and the rest in black). *Imtool* was used for calculating the average size of debris [0-9], every pixel clusters above size 9 was eliminated Again reversed the binary image to the initial form where debris appears in black, cat tool was used to combine results to a single raster file. Raster to poly (polygonise) tool in ArcGIS used to create shape file for extracted debris for Accuracy assessment 16 sample subsets were created for each method based on different criteria's like altitude, presence of streams, type of ice like blue, white, debris mixed areas, presence of island etc. **.** True positive (Correctly identified**)**, false positive (Incorrectly identified**)** and false negatives (Incorrectly rejected**)** were counted manually through visual interpretation. Total area of debris is also calculated for each tile for bias and RMSE Counts from confusion matrix used for calculating parameters for accuracy assessment (Misclassification, False alarms, Accuracy assessment, etc.) best method was selected based on these parameters (Table 2).

From the sample tiles we calculated different parameters like Misclassification, False alarms, Accuracy, False

Positive, False negative, Completeness, Correctness, Quality, Bias, RMSE. The calculations mentioned above were performed manually by comparing extracted debris and reference data. We manually counted number of debris in each tiles for calculation (Table 3).

Table 2. Set of parameters used for robust statistical accuracy analysis of extracted debris features

Accuracy Parameter	Mathematical expression
Misclassification (Mc) (%)	$\frac{\text{No. of unextracted features}}{\text{Total no. of reference features}} \times 100$
False alarms (FA) (%)	$\frac{\text{No. of false extractions}}{\text{No. of total extractions}} \times 100$
Accuracy (Ac) (%)	$100 - \%$ Misclassification
False positive (FP)	No. of extracted features $-$ No. of correctly extracted features
False negative (FN)	No. of reference features – No. of correctly extracted features
Completeness (Ce) (%)	(True Positive/(True Positive + False Negative)) × 100 or (Length of matched reference/Length of Reference) × 100
Correctness (Cr) (%)	(True Positive/(True Positive + False Positive)) × 100 or (Length of Matched Extraction/Length of Extraction) × 100
Quality (Q)	(True Positive ÷ (True Positive + False Positive + False Negative)) × 100

From the tiles we calculated different parameters like Misclassification, False alarms, Accuracy, False Positive, False negative, Completeness, Correctness, Quality, Bias, RMSE. The calculations mentioned above were performed manually by comparing extracted debris and reference data.

4. RESULTS AND DISCUSSION

The results of the classification and performed are given in Table 3. It showed a misclassification percentage of 24.42%, false alarm percentage of 6.27%, accuracy of 75.58%, completeness with 93.73%, correctness of 78.55%, and quality of 40.69%. Figure 5, 6 and 7 show the results obtained from the study. From this, it is clear that extraction by MATLAB showed promising results in case of Accuracy, False alarms, and Misclassification, we also performed studies with other sophisticated software's like eCognition and ENVI even though it managed to get greater accuracy result with MATLAB stands out with less over estimation.

Table 3. Parameters considered for accuracy assessment

Sample number	Misclassification (Mc) (%)	False alarms (FA) (%)	Accuracy (Ac) (%)	Completeness (Ce) (%)	Correctness (Cr) (%)	Quality (Q)
1	21.05	13.89	78.95	86.11	91.72	44.41
2	7.25	6.36	92.75	93.64	94.64	47.07
3	3.14	2.34	96.86	97.66	98.24	48.97
4	0.00	0.00	100.00	100.00	100.00	50.00
5	1.82	12.33	98.18	87.67	98.46	46.38
6	25.12	4.17	74.88	95.83	64.34	38.49
7	14.00	10.26	86.00	89.74	83.33	43.21
8	28.57	5.26	71.43	94.74	75.00	41.86
9	10.00	13.73	90.00	86.27	93.62	44.90
10	42.45	0.00	57.55	100.00	24.36	19.59
11	12.43	10.81	87.57	89.19	61.11	36.26
12	34.52	9.95	65.48	90.05	92.23	45.56
13	55.17	3.70	44.83	96.30	89.04	46.26
14	51.19	0.00	48.81	100.00	3.23	3.13
15	62.50	5.50	37.50	94.50	94.97	47.37
16	21.43	1.97	78.57	98.03	92.55	47.60
Average	**24.42**	**6.27**	**75.58**	**93.73**	**78.55**	**40.69**

Table 3 shows the results of accuracy assessment. The results obtained from this study clearly demonstrate that extraction with MATLAB shows promising results in case of Accuracy, False alarms, and Misclassification. We also

performed studies with other sophisticated software's like eCognition and ENVI even though it managed to get greater accuracy result with MATLAB stands out with less over estimation.

5. CONCLUSION

In this study, we performed pixel-based classification of supraglacial debris using MATLAB's image processing toolbox. It managed to extract debris with accuracy around 70% (Figure 3), but it gave greater completion and false alarm percentage and also less over estimation. The results suggest that clustered debris found at the higher elevated areas and scattered debris with less area and large in number found at the lower elevated areas. Apart from the results obtained, we observed that MATLAB is useful for handling large satellite imagery and for quick processing of large data.

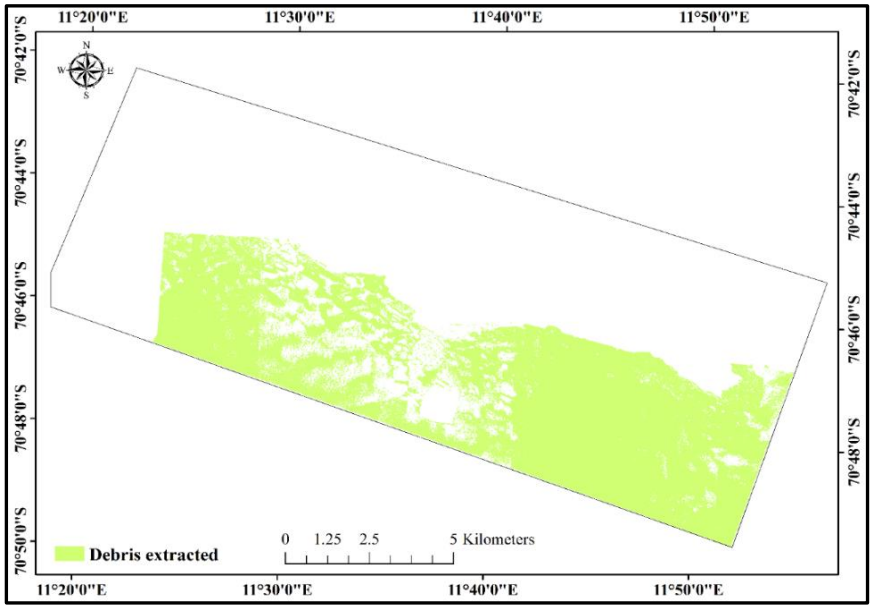

Figure 3. Extracted debris from the study area

ACKNOWLEDGEMENTS

The authors would like to thank DigitalGlobe for providing the imagery used in this study. We also acknowledge Dr. Rajan, former Director, ESSO-NCAOR and Dr. M. Ravichandran, Director, ESSO-NCAOR, for their encouragement and motivation for this research.

REFERENCES

Jawak, S. D., and Luis, A. J., 2015d. Spectral information analysis for the semiautomatic derivation of shallow lake bathymetry using high-resolution multispectral imagery: A case study of Antarctic coastal oasis, International Conference on Water Resources, Coastal And Ocean Engineering (ICWRCOE 2015), Aquatic Procedia 4, 1331-1338**.** DOI:10.1016/j.aqpro.2015.02.173

Jawak, S. D., and Luis, A. J., 2015e. A rapid extraction of water body features from Antarctic coastal oasis using very high-resolution satellite remote sensing data, ICWRCOE 2015, Aquatic Procedia 4, 125-132**.** DOI:10.1016/j.aqpro.2015.02.018

Jawak, S. D., Panditrao, S. N., Luis, A. J., 2014d. Enhanced urban landcover classification for operational change detection study using very high resolution remote sensing data. The International Archives of the Photogrammetry, Remote Sensing and Spatial Information Sciences, Volume XL-8, 2014, ISPRS Technical Commission VIII Symposium, 09–12 December 2014, pp. 773-779. DOI:10.5194/isprsarchives-XL-8-773-2014.

Jawak, S. D., Raut, D. A. and Luis, A. J., 2015f. Iterative spectral index ratio exploration for object-based image analysis of Antarctic coastal oasis using high resolution satellite remote sensing data, ICWRCOE 2015, Aquatic

Procedia 4, 157-164**.** DOI:10.1016/j.aqpro.2015.02.022

Jawak, S.D., and Luis, A.J., 2012. Hyperspatial WorldView-2 Satellite Remote Sensing Data for Polar Geospatial Information Mining of Larsemann Hills, East Antarctica, 11th PORSEC, 05-09 November 2012, Abstract volume, Id: PORSEC2012-24-00006, pp 348. DOI: 10.13140/RG.2.1.3946.8647.

Jawak, S.D., and Luis, A.J., 2014a. Spectral Bands of WorldView-2 Satellite Remote Sensing Data for Semiautomatic Land Cover Extraction in the Antarctic Environment. XXXIII SCAR and 6th Open Science Conference, 25-28 August 2014, Auckland, New Zealand. DOI: 10.13140/RG.2.1.3684.7207.

Jawak, S.D., Devliyal, P., and Luis, A.J., 2015b. A Comprehensive Review on Pixel Oriented and Object Oriented Methods for Information Extraction from Remotely Sensed Satellite Images with a Special Emphasis on Cryospheric Applications. Advances in Remote Sensing 4 (September): 177–95. doi:10.4236/ars.2015.43015.

Jawak, S.D., Khopkar, P.S., Jadhav, S.P., and Luis, A.J., 2013e. Customization of Normalized Difference Snow Index for Extraction of Snow Cover from Cryospheric Surface using WorldView-2 Data, Proceedings of AGSE international conference, 16-19 December, CEPT University, Ahmedabad, India**,** pp. 391-398. ISBN 978-3-943321-12-8**.** DOI: 10.13140/RG.2.1.1325.4246.

Jawak, S.D., Kulkarni, K., and Luis A.J., 2015c. A Review on Extraction of Lakes from Remotely Sensed Optical Satellite Data with a Special Focus on Cryospheric Lakes. J 4 (4): 196–213. doi:10.4236/ars.2015.43016.

Jawak, S.D., Luis, A.J., 2013a. Very-high resolution remotely sensed satellite data for improved land cover extraction of Larsemann Hills, east Antarctica. Journal of Applied Remote Sensing, 0001;7(1):073460. DOI:10.1117/1.JRS.7.073460.

Jawak, S.D., Luis, A.J., 2013b. A comprehensive evaluation of PAN-sharpening algorithms coupled with resampling methods for image synthesis of very high resolution remotely sensed satellite data. Advances in Remote Sensing, Vol. 2 No. 4, pp. 332-344. DOI: 10.4236/ars.2013.24036.

Jawak, S.D., Luis, A.J., 2013c. Improved land cover mapping using high resolution multiangle 8-band WorldView-2 satellite remote sensing data. Journal of Applied Remote Sensing, 7(1), 073573, DOI: 10.1117/1.JRS.7.073573.

Jawak, S.D., Luis, A.J., 2013d. A spectral index ratio-based Antarctic land-cover mapping using hyperspatial 8-band WorldView-2 imagery. Polar Science, Vol. 7, No. 1, pp. 18–38, ISSN 1873-9652, DOI:10.1016/j.polar.2012.12.002.

Jawak, S.D., Luis, A.J., 2014b. A Novel Set of Normalized Difference Snow/Ice Index ratios for Extraction of Snow Cover from the Antarctic Environment using Very High Resolution Satellite Data, XXXIII SCAR and 6th Open Science Conference, 25-28 August 2014, Auckland, New Zealand. DOI: 10.13140/RG.2.1.2636.1441.

Jawak, S.D., Luis, A.J., 2014c. A semiautomatic extraction of Antarctic lake features using WorldView-2 imagery. Photogrammetric Engineering & Remote Sensing, Vol. 80, No. 10, pp. 939-952, DOI: 10.14358/PERS.80.10939.

Jawak, S.D., Luis, A.J., 2015a. Very high resolution satellite imagery for cryospheric geospatial and geoscientific information extraction. XII International Symposium on Antarctic Earth Science (ISAES 2015), Abstract No. S22-5, pp. 479. DOI: 10.13140/RG.2.1.2275.6960.

Jawak, S.D., Luis, A.J., 2016a. High resolution multispectral satellite imagery for extracting bathymetric information of Antarctic shallow lakes. SPIE Asia-Pacific Remote Sensing, New Delhi, India, 4-7 April 2016, Proc. SPIE 9878, Remote Sensing of the Oceans and Inland Waters: Techniques, Applications, and Challenges, 987819, doi:10.1117/12.2222769.

Jawak, S.D., Mathew, J., 2011. Semi-automatic extraction of water bodies and roads from high resolution QuickBird satellite data, Proceedings of Geospatial World Forum. PN-263, pp.247-257, DOI: 10.13140/RG.2.1.3291.5043.

Jawak, S.D., Yogesh Palanivel, V., Luis, A.J., 2016b. Semi-automatic extraction of supra-glacial features using fuzzy logic approach for object-oriented classification on WorldView-2 imagery. SPIE Asia-Pacific Remote Sensing 2016. Proc. SPIE 9880, Multispectral, Hyperspectral, and Ultraspectral Remote Sensing Technology, Techniques and Applications VI, 98801S, doi:10.1117/12.2223024.

Juen, M., C. Mayer, A. Lambrecht, H. Han, and S. Liu., 2014. Impact of Varying Debris Cover Thickness on Ablation: A Case Study for Koxkar Glacier in the Tien Shan. Cryosphere 8 (2): 377–86. doi:10.5194/tc-8-377-2014.

Lillesand R.W., T M and Kiefer., 2015. Remote Sensing and Image Interpretation Seventh Ed. John Wiley and Sons, Inc., New York.

Müller, F, and K Scherler., 1966. Introduction to the World Glacier Inventory. IAHS Publication. http://iahs.info/redbooks/a126/iahs_126_0000Intro.pdf.